# Four key signaling pathways mediating chemotaxis in *Dictyostelium discoideum*

Douwe M. Veltman, Ineke Keizer-Gunnik, and Peter J.M. Van Haastert

Department of Molecular Cell Biology, University of Groningen, 9751 NN Haren, Netherlands

Chemotaxis is the ability of cells to move in the direction of an external gradient of signaling molecules. Cells are guided by actin-filled protrusions in the front, whereas myosin filaments retract the rear of the cell. Previous work demonstrated that chemotaxis of unpolarized amoeboid *Dictyostelium discoideum* cells is mediated by two parallel pathways, phosphoinositide-3-kinase (PI3K) and phospholipase A2 (PLA2). Here, we show that polarized cells exhibit very good chemotaxis with inhibited PI3K and PLA2 activity. Using genetic screens, we demonstrate that this activity is mediated by a soluble guanylyl cyclase, providing two signals. The protein localizes to the leading edge where it interacts with actin filaments, whereas the cyclic guanosine monophosphate product induces myosin filaments in the rear of the cell. We conclude that chemotaxis is mediated by multiple signaling pathways regulating protrusions at the front and rear of the cell. Cells that express only rear activity are polarized but do not exhibit chemotaxis, whereas cells with only front signaling are unpolarized but undergo chemotaxis.

## Introduction

Chemotaxis is a pivotal response of many cell types to external spatial cues. It plays important roles in diverse functions such as finding nutrients in prokaryotes, forming multicellular structures in protozoa, tracking bacterial infections in neutrophils, and organizing the embryonic cells in metazoa (Baggiolini, 1998; Campbell and Butcher, 2000; Crone and Lee, 2002). In *Dictyostelium discoideum* cells, extracellular cAMP functions as a chemoattractant that is detected by specific G protein–coupled surface receptors. Chemotaxis is achieved by coupling gradient sensing to basic cell movement. Pseudopod extension at the leading edge is mediated by the formation of new actin filaments, whereas actomyosin filaments in the rear of the cell inhibit pseudopod formation and retract the uropod.

We are beginning to understand the signals that mediate chemotaxis (Van Haastert and Devreotes, 2004; Affolter and Weijer, 2005; Franca-Koh et al., 2007). Phosphatidylinositol (3,4,5)-trisphosphate ($PIP_3$) is a very strong candidate to mediate directional sensing in neutrophils and *D. discoideum*. $PIP_3$ is formed at the side of the cell closest to the source of chemoattractant (Parent et al., 1998; Hirsch et al., 2000; Servant et al., 2000; Funamoto et al., 2002; Iijima and Devreotes, 2002). Unexpectedly, inhibition of phosphoinositide-3-kinase-kinase (PI3K) has only moderate effects on chemotaxis in *D. discoideum* (Funamoto et al., 2002; Iijima and Devreotes, 2002; Postma et al., 2004; Loovers et al., 2006; Takeda et al., 2007) and mammalian cells (Wang et al., 2002; Ward, 2004, 2006). Recently, all five genes encoding type I PI3Ks were inactivated (Hoeller and Kay, 2007); cells exhibit nearly normal chemotaxis in steep cAMP gradients, demonstrating that $PIP_3$ signaling is not essential for chemotaxis and that other parallel pathways are present. A phospholipase A2 (PLA2) pathway mediating chemotaxis in *pi3k* null cells was identified independently using genetic (Chen et al., 2007) and pharmacological approaches (van Haastert et al., 2007). Inhibition of either the PI3K or PLA2 pathway had minor effects, whereas the inactivation of both pathways blocked chemotaxis.

The experiments described above were performed with ~5-h starved cells that are amoeboid and unpolarized. When the gradient of cAMP is reversed, these cells extend a pseudopod from the rear and cells revert direction with a new front. Cells starved for longer periods become highly polarized. They do not only adopt an elongated shape but also obtain a front–rear axis of graded sensitivity to chemotactic signals. When the gradient of cAMP is reversed, 7-h starved cells extend a pseudopod at the front and cells gradually turn around (Swanson and Taylor, 1982; Chen et al., 2003). We show here that inhibition of PI3K and PLA2 dramatically inhibits chemotaxis of 5-h starved

Correspondence to P.J.M. Van Haastert: P.J.M.van.haastert@rug.nl

Abbreviations used in this paper: BPB, bromophenacyl bromide; cGMP, cyclic guanosine monophosphate; $IP_3$, inositol triphosphate; PI3K, phosphoinositide-3-kinase; $PIP_3$, phosphatidylinositol (3,4,5)-trisphosphate; PLA2, phospholipase A2; sGC, soluble guanylyl cyclase.

The online version of this paper contains supplemental material.

THE JOURNAL OF CELL BIOLOGY

Figure 1. **Chemotaxis during development when cells become polarized.** (A) Chemotaxis to 1 µM cAMP in the absence of PI3K and PLA2 activity (inhibited with LY and BPB or removed by disruption of the encoding genes). Cells without PI3K and PLA2 activity exhibit poor chemotaxis at 5 h of development but very strong chemotaxis at 7 h of development. The chemotactic response of cells that do have PI3K and/or PLA2 activity (WT, *pi3k* null, and *pla2* null) is indicated by the horizontal gray bar. The data presented are the means and SEM of at least three independent measurements. (B) Morphology of 5- and 7-h starved cells expressing myosin-II–RFP and LimEΔcoil-GFP detecting actin filaments. Bar, 10 µm.
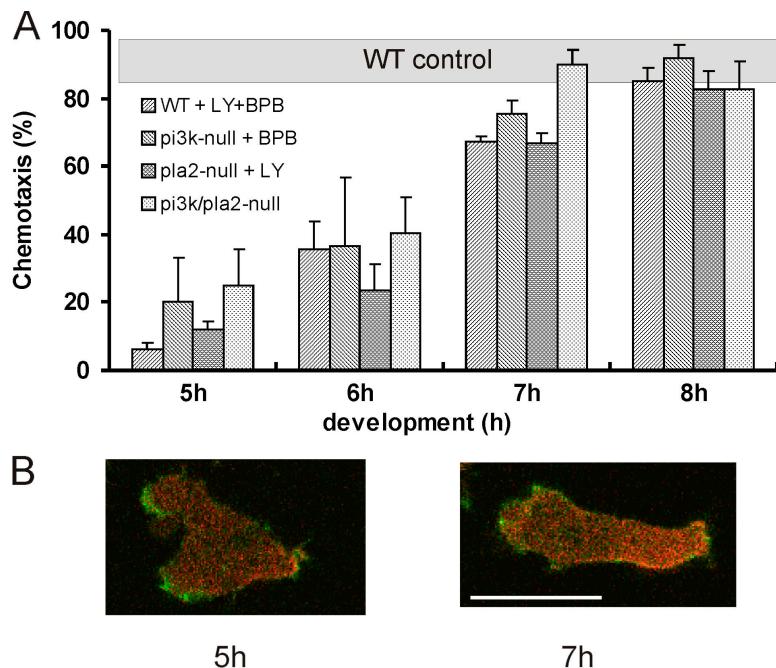
cells but has little effect at later stages of *D. discoideum* development; 7-h starved *pi3k/pla2* null cells exhibit excellent chemotaxis. This could imply a third signaling pathway that becomes operational in polarized cells. We tested several mutants for the ability to exhibit chemotaxis in the absence of PI3K and PLA2 activity, showing that adenylyl cyclase, TORC2/PKBR1, and PLC/ inositol triphosphate (IP₃)/Ca²⁺ signaling are not essential for PI3K/PLA2-independent chemotaxis. In contrast, deletion of a soluble guanylyl cyclase (sGC) blocks chemotaxis of polarized cells. Mutational analysis reveals that sGC provides two signals. The protein localizes to the leading edge where it interacts with actin filaments, whereas the cyclic guanosine monophosphate (cGMP) product induces myosin filaments in the rear of the cell. We conclude that chemotaxis is mediated by four pathways, PI3K, PLA2, sGC protein, and cGMP.

## Results and discussion

Upon starvation, *D. discoideum* cells become chemotactic to cAMP. Because cAMP is secreted by the cells, chemotaxis induces the cells to aggregate and form a multicellular structure that develops into a fruiting body with dead stalk cells and viable spores. Cells starved for 5 h are unpolarized and extend pseudopodia in all directions. These cells are fully competent to chemotax toward cAMP, which induces actin filaments in the front and myosin filaments in the rear of the cell (Fig. 1). Chemotaxis is blocked upon inhibition of both PI3K and PLA2 activity, either by deletion of the encoding genes or by pharmacological inhibition of the enzyme activities with LY294002 (LY) and p–bromophenacyl bromide (BPB), respectively (Fig. 1 A; Chen et al., 2007; van Haastert et al., 2007). Cells starved for 7 h acquire a strong internal polarity and are very elongated in the absence or presence of a cAMP gradient (Fig. 1 B). Surprisingly, inhibition of PI3K and PLA2 activity has little effect on chemotaxis. Apparently, PI3K and PLA2 activity mediate all chemotaxis in

unpolarized cells, whereas intrinsic polarization of the cells allows cells to chemotax using an alternative pathway.

We investigated several mutant cells with deletion of a specific signaling pathway to perform chemotaxis in the absence of PI3K and PLA2 activity after 7 h of starvation. The results of Fig. 2 A show that wild-type cells chemotax nearly equally well to cAMP in the absence or presence of the PI3K and PLA2 inhibitors (LY + BPB inhibit chemotaxis only 13 ± 8%). LY + BPB does not inhibit chemotaxis of cells with a deletion of PI3K, PLA2, the PIP3 target Akt/PKB, the TORC2 target PKBR1, phospholipase C activity, adenylyl cyclase activity, and the IP₃ receptor (Fig. 2 A). Apparently, PKB, intracellular cAMP, and Ca²⁺ are not required for chemotaxis of polarized cells in the presence of LY + BPB. Cells that lack both PIP3-dependent Akt/PKB and TORC2-dependent PKBR1 exhibit reduced chemotaxis compared with wild-type cells but this chemotactic activity is not further reduced by LY + BPB. Similar observations were made in *pia* null cells that lack the homologue of AVO3/Rictor in the TORC2 complex, which suggests that TORC2 signaling may have a general contribution to chemotaxis or may largely overlap with PI3K/PLA2 signaling but is not responsible for the PI3K- and PLA2-independent chemotaxis of 7-h starved cells. In contrast, deletion of the genes encoding the two guanylyl cyclases GCA and sGC (*gc* null cells; Roelofs and van Haastert, 2002) largely blocks chemotaxis in the presence of LY + BPB. Cells with a deletion of the cGMP target GbpC also fail to exhibit good chemotaxis in the presence of LY + BPB, which suggests that a cGMP signaling pathway mediates chemotaxis of polarized cells. It should be noted that 7-h starved *gc* null or *gbpc* null cells exhibit good chemotaxis in the presence of either LY or BPB (unpublished data), demonstrating that PI3K or PLA2 signaling can mediate chemotaxis in these cells.

Chemotaxis is a combination of motility and directionality of the movement. These parameters were determined in well-defined cAMP gradients produced in a modified Zigmond

A

B
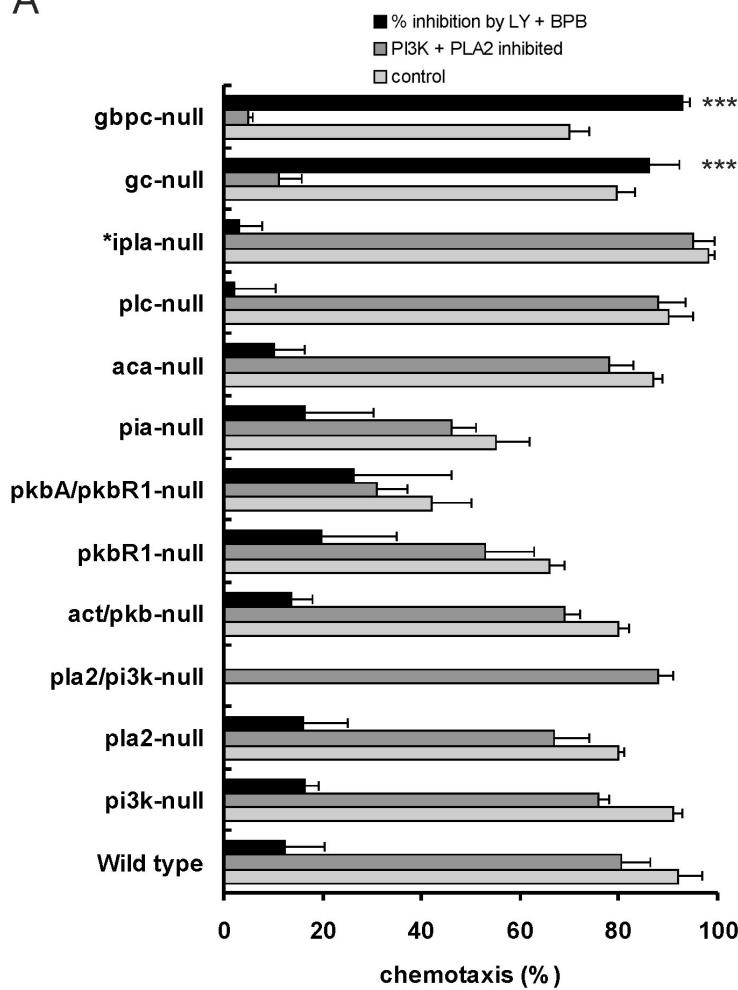
Figure 2. **PI3K- and PLA2-independent chemotaxis in signal transduction mutants.** (A) Chemotaxis to 1 μM cAMP was measured in 7-h starved cells in the absence (control) or presence of LY + BPB (PI3K and PLA2 inhibited). In wild-type cells and many mutants, LY + BPB does not inhibit chemotaxis by >15%, but in the guanylyl cyclase *gc* null and the cGMP target protein *gbpc* null cells, LY + BPB gives strong inhibition of chemotaxis. The asterisk indicates that the *ipla* null cells have a disrupted gene encoding the IP$_3$ receptor and were assayed in the presence of the PLC-inhibitor U23122 (10 μM) and EGTA (10 mM) to block Ca$^{2+}$ uptake and intracellular release. ***, the difference with wild-type is significant at P < 0.001. (B) Chemotaxis was measured in 7-h starved cells toward different concentrations of cAMP. The results show that inhibition of PI3K and PLA2 or guanylyl cyclases lead to a mild inhibition of chemotaxis, whereas chemotaxis is strongly reduced when all three pathways are inhibited. The data presented are the means and SEM of at least three independent measurements.
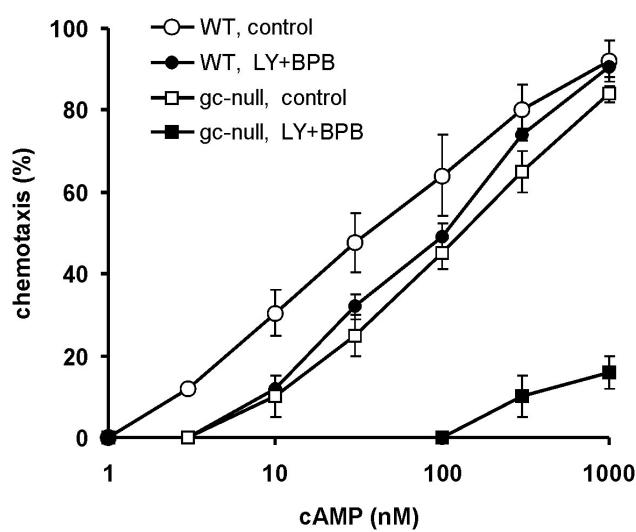
chamber (Table I). In this assay, wild-type cells have a chemotaxis index of ∼0.7 and a speed of ∼9 μm/min. The chemotaxis index and speed of 7-h starved *gc* null cells is only slightly smaller than that of wild-type cells. Inhibition of PI3K and PLA2 activity in these *gc* null cells has no effect on the speed of the cells but dramatically reduces the chemotaxis index. This low directionality

is also associated with a reduction of the persistence of the trajectories and an increase of the roundness of the cells.

GCA is a 12-transmembrane guanylyl cyclase that is active during early starvation, whereas the sGC provides nearly all cAMP-stimulated cGMP production in 7-h starved cells (Roelofs and van Haastert, 2002), and the cGMP response is very

Table I. **Chemotaxis of cells lacking PI3K, PLA2, and sGC**

| Strain | Chemotaxis | | Speed | Persistence | Roundness |
|---|---|---|---|---|---|
| | % | CI | μm/min | | |
| Wild type | 92 ± 5 | 0.73 ± 0.05 | 9.1 ± 0.7 | 0.90 ± 0.03 | 0.30 ± 0.023 |
| Gc null | 80 ± 3 | 0.64 ± 0.03 | 7.8 ± 0.4 | 0.76 ± 0.02 | 0.33 ± 0.036 |
| Gc null + LY + BPB | 11 ± 5 | 0.19 ± 0.04 | 7.9 ± 0.3 | 0.43 ± 0.02 | 0.54 ± 0.030 |
| sgc/pla2 null | 82 ± 9 | 0.74 ± 0.02 | 7.6 ± 0.5 | 0.85 ± 0.01 | 0.36 ± 0.036 |
| sgc/pla2 null + LY | 10 ± 4 | 0.22 ± 0.04 | 5.0 ± 0.4 | 0.43 ± 0.03 | 0.46 ± 0.036 |

The chemotaxis index (CI), speed, persistence (displacement divided by the length of the path), and roundness (short axis divided by the long axis of a cell considered as an ellipse) were determined for the conditions indicated using the modified Zigmond chamber with 1 μM cAMP in the source. LY is the PI3K inhibitor LY294002; BPB is the PLA2 inhibitor p-BPB. The data shown are the means and SEM of 24–33 cells. The first chemotaxis column shows the chemotactic activity measured with the population assay.

similar to that of 5-h starved cells (Fig. 3 C). In 7-h starved cells with LY + BPB, deletion of only *gca* has no effect and deletion of only *sgc* completely blocks chemotaxis, whereas expression of sGC in the *gca/sgc* null restores all chemotaxis (see following paragraph; Fig. 3 E), indicating that sGC and not GCA is essential for PI3K- and PLA2-independent chemotaxis. To further explore chemotaxis of 7-h starved cells, we made a cell line lacking both sGC and PLA2. On nonnutrient agar plates, these *sgc/pla2* null cells develop as wild-type cells with pulsatile cell aggregation, which suggests good cAMP oscillations and chemotaxis (unpublished data). In the small population chemotaxis assay, *sgc/pla2* null cells exhibit excellent chemotaxis, which is nearly completely inhibited by LY (Table I). In the modified Zigmond chamber, *sgc/pla2* null cells move with a speed and chemotaxis index that is slightly less than that of wild-type cells. The addition of 50 μM LY induces a small reduction of the cell speed but a strong decline of the chemotaxis index of *sgc/pla2* null cells, similar to the effect of LY + BPB in *gc*-null cells (Table I and Videos 1 and 2, available at http://www.jcb.org/cgi/content/full/jcb.200709180/DC1).

The large 280-kD sGC protein has an N-terminal ∼1,000 amino acids domain that is essential and sufficient for localization of the sGC protein to the filamentous actin network at the leading edge, whereas the central ∼600 amino acids are essential for catalytic activity (Veltman and Van Haastert, 2006). A mutant expressing sGC with a point mutation of the catalytic D1106A (sGCΔCat) has lost all guanylyl cyclase activity (Fig. 3 C) but still localizes to the leading edge of cells in a cAMP gradient in the absence or presence of LY + BPB (Fig. 3 A). In contrast, a mutant with a deletion of the N-terminal domain (sGCΔN) is entirely cytosolic but retains normal cAMP-stimulated guanylyl cyclase activity. Coexpression of sGCΔCat-GFP and the F-actin–binding protein LimEΔcoil-RFP reveals colocalization of the proteins in LY + BPB (Fig. 3 B), which suggests that sGC protein may provide front signaling in the absence of PI3K and PLA2.

For the function of cGMP product, we refer to the previously identified cGMP signaling pathway in *D. discoideum* (Bosgraaf et al., 2002). The cGMP target protein GbpC mediates myosin filament formation at the side and in the rear of the cell, leading to inhibition of pseudopod extension at these sides as well as retraction of the uropod. *D. discoideum* cells may extend pseudopodia by splitting of an existing pseudopod (Andrew and Insall, 2007) or by forming a pseudopod from areas of the cell previously devoid of pseudopod activity (de novo pseudopod). Cells were placed in a cAMP gradient delivered by the modified Zigmond chamber. We recorded the formation of pseudopodia in the front or back half of the cell, their formation by pseudopod splitting or de novo, and whether they are retracted or maintained. The four cell lines show approximately the same global rate of pseudopod extensions (between 2.1 and 2.5 pseudopodia per min; Fig. 3 D). Wild-type cells and *gc* null cells expressing sGC predominantly extend pseudopodia in a cAMP gradient at the front by the splitting of existing pseudopodia. In contrast, *gc* null cells exhibit a strong increase of de novo pseudopodia, both in the front and, somewhat stronger, in the back of the cell. Because pseudopod splitting is absent in the back, the consequence of global inhibition of de novo pseudopodia is the near absence of pseudopod extension from the back of the cell. Thus, in a cAMP gradient, only ∼4% of all pseudopodia are formed in the back of wild-type cells, which is 23.2 ± 2.2% of all pseudopodia in *gc* null cells, almost as many as wild-type cells in buffer (24.9 ± 4.3%). The distribution of pseudopodia in sGCΔCat is very similar to that of *gc* null cells, whereas the distribution in sGCΔN resembles that of wild-type cells. The data indicate that the predominant defect of *gc* null cells is a failure to suppress de novo pseudopodia in the back of the cell, which is caused by the lack of cGMP production and does not depend on the localization of the sGC protein. In conclusion, the sGC protein interacts with F-actin in the front of the cell, whereas the produced cGMP inhibits the extension of lateral pseudopodia.

We analyzed the contribution of sGC protein and cGMP product to chemotaxis when PI3K and PLA2 signaling is absent (Fig. 3 E). Expression of the full-length sGC completely restores chemotaxis of 7-h *gc* null cells in the presence of LY + BPB. Expression of unlocalized but catalytic active sGCΔN in *gc* null cells does not restore chemotaxis, which indicates that cGMP and suppression of pseudopodia in the rear of the cell are not sufficient for chemotaxis. In contrast, expression of the catalytic inactive sGCΔCat that still localizes to the leading edge can partly restore chemotaxis of 7-h *gc* null cells in the presence of LY + BPB. Previous studies have shown that the AAA-ATPase in the C-terminal domain of sGC is essential is the activity of sGCΔCat. Protein structures can be modified by AAA-ATPase domains, providing a possible mechanism how sGC protein may function at the leading edge (Veltman and Van Haastert, 2006).

The results suggest that chemotaxis in *D. discoideum* is mediated by four pathways: PI3K, PLA2, sGC protein, and cGMP.
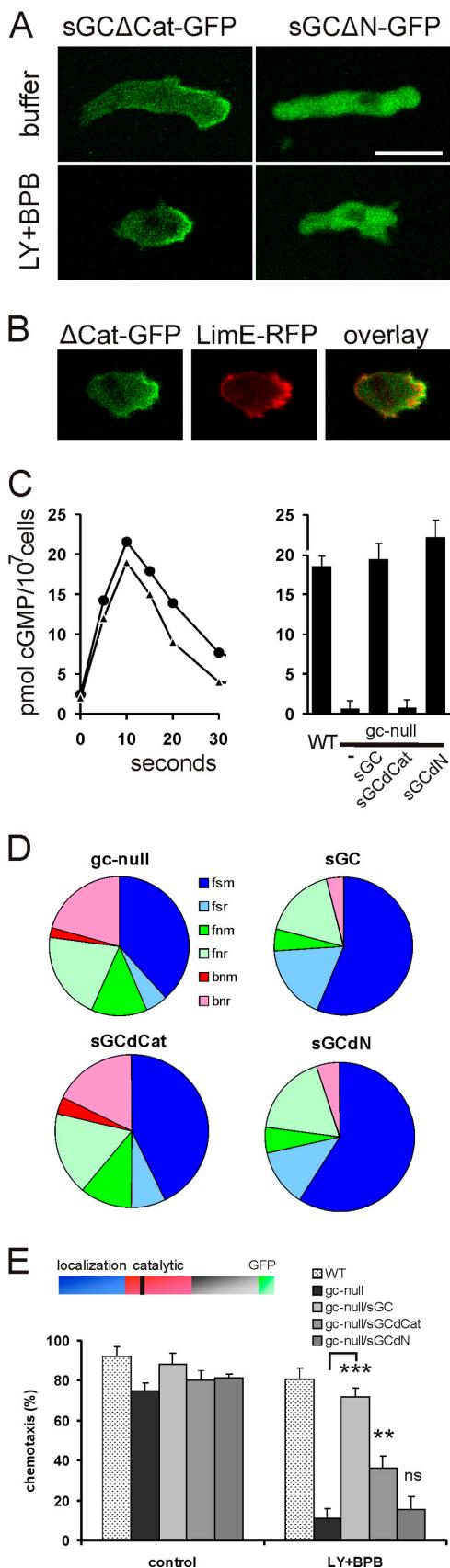
The activation mechanism of PLA2 is not yet known but the other pathways are activated by cAMP through the heterotrimeric G protein $G\alpha2\beta\gamma$ and RasC and/or RasG proteins (Bolourani et al., 2006). Cells starved for 7 h are highly polarized in buffer with a clear front that is more sensitive to cAMP than the rear of the cell (Swanson and Taylor, 1982). In these polarized cells, sGC can mediate chemotaxis in the absence of PI3K and PLA2 activity. Because 5-h starved unpolarized cells exhibit the same activation of sGC as 7-h starved cells, it suggests that intrinsic polarization is a prerequisite for strong chemotaxis by sGC. The functions of the signaling pathways may be interpreted in the context of cell polarity with distinct front and rear. Two pathways, PI3K and sGC protein, most likely function at the front of the cell. The cGMP pathway predominantly regulates myosin at the side and in the rear of the cell, similar to the role of Rho-kinase in mammalian cells (Xu et al., 2003). The mechanism of action of the PLA2 pathway is not well understood. PLA2 is cytosolic, and addition of the PLA2 product arachidonic acid to the extracellular medium partly restores the defect of *pla2* null cells (Chen et al., 2007), which suggests that PLA2 may regulate both front and rear. The results suggest a strong synergy between front and rear signaling. Rear signaling in the absence of front signaling (*gc* null/sGCΔN in the presence of LY + BPB) does not provide chemotactic activity. Although these cells exhibit reduced pseudopod extensions in the rear and have a polarized shape, the pseudopod extensions and retractions at the front are apparently not sufficiently biased by the chemoattractant gradient to provide strong chemotaxis. Front signaling alone can provide significant chemotaxis, as observed in *gc* null/sGCΔCat in the presence of LY + BPB. Thus, the leading edge alone can align with the gradient but chemotaxis is not very efficient because many pseudopodia are extended at the rear of the cell.

The four key signaling pathways identified here are most likely supported by other pathways to provide a full chemotactic response. However, as chemotaxis is nearly completely blocked in

**Figure 3. Two functions of sGC: as a protein and as an enzyme producing cGMP.** The strains used were *gc* null cells, *gc* null cells expressing full-length sGC, *gc* null cells expressing sGCΔN with a deletion of the N-terminal 877 amino acids, and *gc* null cells expressing sGCΔCat with a point mutation

rendering the protein catalytic inactive. (A) Localization of sCGΔCat-GFP and sGCΔN-GFP in a cAMP gradient in the absence or presence of LY + BPB. (B) Colocalization of sCGΔCat-GFP and LimEΔcoil-RFP in a cAMP gradient in the presence of LY + BPB (same cell as in A). Bar, 10 μm. (C) cGMP response. (left) The kinetics of the response of wild-type cells at 5 (circle) and 7 h (triangle) of development. (right) The cGMP response at 12 s after stimulation of the indicated strains with 1 μM cAMP. The data shown are the means and SD of three determinations. (D) Formation of pseudopodia in cAMP gradients. Cells were placed in a gradient delivered by a modified Zigmond chamber with 1 μM cAMP at the source. Videos were recorded at a rate of one frame per second and analyzed for where and how pseudopodia are extended and retracted. We recorded the formation of pseudopodia in the front (f) or back (b) half of the cell, their formation by splitting of an existing pseudopod (s) or de novo from an area devoid of pseudopod activity (n), and whether pseudopodia are retracted (r) or maintained (m). From the eight categories possible, we never observed splitting in the back of the cell, leaving the six categories as presented. The rate of pseudopod formation per min is $2.04 \pm 0.31$ for sGC, $2.13 \pm 0.23$ for sGCΔN, $2.46 \pm 0.38$ for sGCΔCat, and $2.45 \pm 0.30$ for *gc* null cells. The data shown are the means and SE for 36 pseudopodia from three independent experiments. (E) Chemotaxis to 1 μM cAMP was measured with the small population assay. The difference between *gc* null cells and *gc* null cells expressing mutant sGC is significant at $P < 0.001$ (***), at $P < 0.01$ (**), or is not significant at $P > 0.5$ (ns). The data presented are the means and SEM of at least three independent measurements.

cells lacking PI3K, PLA2, and sGC, the other pathways on their own are not sufficient to provide directional signaling. These pathways, such as activation of PKBR1, PLC, intracellular cAMP, and Ca$^{2+}$, may regulate pseudopodia globally, or they may use PI3K, PLA2, or sGC to express their effect at the front or rear of the cell. Indeed, it has been proposed that PLC activity stimulates the PIP$_3$ response (Keizer-Gunnink et al., 2007; van Haastert et al., 2007), whereas Ca$^{2+}$ may stimulate the PLA2 and inhibits the sGC pathway (Valkema and Van Haastert, 1992; Roelofs and van Haastert, 2002).

The identification of four key pathways regulating chemotaxis provides important tools to dissect the complex signaling network that together may be regarded as the molecular compass of navigating cells. By creating cell lines in which three pathways are inactivated, the role of the fourth pathway can be investigated in large detail. In this study, we made a start with sGC protein using gc null/sGCΔCat cells in the presence of LY + BPB. The function of the poorly understood PLA2 pathway can be elucidated in cells lacking all PI3Ks and guanylyl cyclases. Such cell lines are also instrumental to address eminent questions on chemotaxis. What is the gradient sensing mechanism? How is the cAMP gradient amplified during chemotaxis? What is the contribution of each signaling pathway to the regulation of pseudopodia? Wild-type cells respond to a 5% difference in receptor activation across the cell with 80% accuracy to move in the direction of the gradient, clearly showing amplification of the signal (Mato et al., 1975; Van Haastert and Postma, 2007). In wild-type cells, the gradient of G protein activation is not amplified (Janetopoulos et al., 2001), whereas the gradient of PI3K activation is amplified about threefold (Janetopoulos et al., 2004). In wild-type cells, it is difficult to discriminate between primary events that depend on the gradient of receptor activation and secondary events that are regulated by one of the many positive feedback loops, such as PI3K-actin, Ras-actin, and PI3K-Ras positive feedback loops (Sasaki et al., 2007). In a cell lacking all PI3K, PLA2, and sGC activity, the primary gradient-responding events are expected to be present as in wild-type cells, whereas all positive feedback loops via one of these signaling pathways are inhibited. Furthermore, many proteins accumulate at the leading edge of a chemotaxing cell (Affolter and Weijer, 2005; Charest and Firtel, 2007; Franca-Koh et al., 2007). By investigating the spatial-temporal activation of these molecules in cells lacking all four chemotactic signaling pathways, we may identify the components of the core sensory transduction pathway and its internal spatial-temporal amplification, whereas the contribution of PI3K, PLA2, and sGC signaling can be investigated using cells expressing only one or combinations of these pathways.

The recent observations on chemotaxis in *D. discoideum* demonstrate a surprising variety of signaling molecules and cellular responses. Comparison of chemotaxis in bacteria and eukaryotes suggests that during evolution, chemotaxis in bacteria has been improved by fine tuning the relatively simple cascade for temporal signaling (Baker et al., 2006; Bray et al., 2007), whereas in eukaryotes, additional signaling systems have been implemented to gradually improve chemotaxis to the limit of what is physically possible in spatial sensing.

# Materials and methods

The strains used were wild-type AX3, *pi3k* null strain GMP1 with a deletion of *pi3k1* and *pi3k2* genes (Funamoto et al., 2001), *pla2* null with a deletion of the *plaA* gene (Chen et al., 2007), *pi3k/pla2* null cells (Chen et al., 2007), *Akt/pkb* null cells with a deletion of *pkbA* (Meili et al., 2000), *pkbR1* null cells (Lee et al., 2005), *plc* null strain 1.19 (Drayer et al., 1995), *aca* null cells (Pitt et al., 1992), *ipla* null strain HM1038 with a deletion of *iplA* encoding the IP$_3$ receptor (Traynor et al., 2000), *gc* null cells with a deletion of *gca* and *sgc* (Veltman and Van Haastert, 2006), *sgc* null cells (Roelofs et al., 2001), *gbpc* null cells (Bosgraaf et al., 2002), *gc* null/sGC cells expressing full-length sGC in *gc* null cells, *gc* null/sGCΔCat expressing sGC-D1106A in *gc* null cells, *gc* null/sGCΔN expressing sGC with the N-terminal deletion of 877 amino acids in *gc* null cells (Veltman and Van Haastert, 2006), and *gbpc* null/GbpC expressing full-length GbpC in *gbpc* null cells. The *sgc/pla2* null cells were obtained by inactivation of the *sgc* gene in *pla2* null cells and identified by PCR as described previously (Veltman and Van Haastert, 2006). Five independent disruptants were tested for chemotaxis with the population assay; clone C5 was used in the modified Zigmond chamber. Cells were grown in HG5 medium (contains per liter: 14.3 g oxoid peptone, 7.15 g bacto yeast extract, 1.36 g Na$_2$HPO$_4$ × 12 H$_2$O, 0.49 g KH$_2$PO$_4$, and 10.0 g glucose).

Chemotaxis was measured with the small population assay (Konijn, 1970; van Haastert et al., 2007). Cells that produce strong autonomous cAMP signaling (wild-type AX3, *pla2* null, *plc* null, *ipla* null, *gc* null, *gbpc* null, and *sgc/pla2* null cells) were starved on nonnutrient agar (11 mM KH$_2$PO$_4$, 2.8 mM Na$_2$HPO$_4$, and 15 g/liter agar) for 7 h, whereas cells with poor autonomous cAMP signaling (*aca* null, *pi3k* null, *pia* null, *akt/pkb* null, and *pkbr1* null cells) were starved in suspension, with 100 nM cAMP pulses added every 5 min starting after 2 h of starvation. The chemotaxis assays were performed in the wells of a 6-well plate with 1 ml nonnutrient hydrophobic agar (11 mM KH$_2$PO$_4$, 2.8 mM Na$_2$HPO$_4$, and 7 g/liter hydrophobic agar) containing 50 µM LY294002 and/or 2 µM BPB (van Haastert et al., 2007). Droplets of ∼0.1 µl of 7-h starved cells (6 × 10$^6$ cells/ml) were placed on the agar. After 30 min, chemotaxis toward cAMP was tested by placing a second 0.1-µl droplet with 1,000 nM cAMP next to the droplet of cells. The distribution of the cells in the droplet was observed about every 10 min during 90 min. Chemotaxis of cells within a droplet was scored positive when the cell density at the cAMP side was at least twice as high compared with the opposite side of the droplet (Konijn, 1970). Some mutants respond faster (*plc* null) or slower (*pi3k* null) than wild-type cells. Recorded is the fraction of droplets scored positive, averaged over three successive observations at and around the moment of the maximal response. The data presented are the means and standard error of the means of at least three independent measurements on different days. Chemotaxis was also determined with a modified Zigmond chamber with 1 µM cAMP in the source, essentially as described previously (Veltman and Van Haastert, 2006).

Digital images of cells in PB at room temperature were recorded at a rate of 1 frames/s using an inverted light microscope (Type CK40) with a LWD A240 20× numerical aperture 0.4 objective (both from Olympus) fitted with a charged-coil device camera (TK-C1381; JVC). Digital images were captured on a PC using VirtualDub software (http://www.virtualdub.org) and Indeo video 5.10 compression (Ligos Corporation). The field of observation is 358 × 269 µm. The chemotaxis index, speed, and persistence was determined at an interval of 30 s; the roundness of the cell, defined as the ratio of the short/long axis of an ellipse, was determined as described previously (Loovers et al., 2006). The videos were also used to determine the number of pseudopodia that originate in the front and rear half of the cell. The front half is defined as the half of the cell directed toward the cAMP gradient. We also determined whether these pseudopodia are formed by splitting of an existing pseudopod or from an area devoid of pseudopod activity as defined previously (Andrew and Insall, 2007). The cGMP response was determined as described previously (Veltman and Van Haastert, 2006).

Confocal images were recorded using a confocal laser scanning microscope (LSM 510 META-NLO; Carl Zeiss, Inc.) equipped with a Plan-Apochromatic 63× numerical aperture 1.4 objective (Carl Zeiss, Inc.). For excitation of GFP and mRFP-mars, a 488-nm argon/krypton laser and a 543-nm helium laser (Lasos) were used, respectively. Fluorescent light was filtered through a BP500-530 (GFP) or IR LP560 (mRFP-mars) filter and detected by a photo multiplier tube (Hamamatsu).

### Online supplemental material
Video 1 shows chemotaxis of *sgc/pla2* null cells in a Zigmond chamber. Video 2 shows chemotaxis of *sgc/pla2* null cells in the presence of 50 µM LY294002. Online supplemental materials is available at http://www.jcb.org/cgi/content/full/jcb.200709180/DC1.

# References

Affolter, M., and C.J. Weijer. 2005. Signaling to cytoskeletal dynamics during chemotaxis. *Dev. Cell.* 9:19–34.

Andrew, N., and R.H. Insall. 2007. Chemotaxis in shallow gradients is mediated independently of PtdIns 3-kinase by biased choices between random protrusions. *Nat. Cell Biol.* 9:193–200.

Baggiolini, M. 1998. Chemokines and leukocyte traffic. *Nature.* 392:565–568.

Baker, M.D., P.M. Wolanin, and J.B. Stock. 2006. Signal transduction in bacterial chemotaxis. *Bioessays.* 28:9–22.

Bolourani, P., G.B. Spiegelman, and G. Weeks. 2006. Delineation of the roles played by RasG and RasC in cAMP-dependent signal transduction during the early development of *Dictyostelium discoideum. Mol. Biol. Cell.* 17:4543–4550.

Bosgraaf, L., H. Russcher, J.L. Smith, D. Wessels, D.R. Soll, and P.J.M. Van Haastert. 2002. A novel cGMP signalling pathway mediating myosin phosphorylation and chemotaxis in *Dictyostelium. EMBO J.* 21:4560–4570.

Bray, D., M.D. Levin, and K. Lipkow. 2007. The chemotactic behavior of computer-based surrogate bacteria. *Curr. Biol.* 17:12–19.

Campbell, J.J., and E.C. Butcher. 2000. Chemokines in tissue-specific and microenvironment-specific lymphocyte homing. *Curr. Opin. Immunol.* 12:336–341.

Charest, P.G., and R.A. Firtel. 2007. Big roles for small GTPases in the control of directed cell movement. *Biochem. J.* 401:377–390.

Chen, L., C. Janetopoulos, Y.E. Huang, M. Iijima, J. Borleis, and P.N. Devreotes. 2003. Two phases of actin polymerization display different dependencies on PI(3,4,5)P3 accumulation and have unique roles during chemotaxis. *Mol. Biol. Cell.* 14:5028–5037.

Chen, L., M. Iijima, M. Tang, M.A. Landree, Y.E. Huang, Y. Xiong, P.A. Iglesias, and P.N. Devreotes. 2007. PLA2 and PI3K/PTEN pathways act in parallel to mediate chemotaxis. *Dev. Cell.* 12:603–614.

Crone, S.A., and K.F. Lee. 2002. The bound leading the bound: target-derived receptors act as guidance cues. *Neuron.* 36:333–335.

Drayer, A.L., M.E. Meima, M.W.M. Derks, R. Tuik, and P.J.M. van Haastert. 1995. Mutation of an EF-hand Ca2+-binding motif in phospholipase C of *Dictyostelium discoideum*: inhibition of activity but no effect on Ca2+-dependence. *Biochem. J.* 311:505–510.

Franca-Koh, J., Y. Kamimura, and P.N. Devreotes. 2007. Leading-edge research: PtdIns(3,4,5)P(3) and directed migration. *Nat. Cell Biol.* 9:15–17.

Funamoto, S., K. Milan, R. Meili, and R.A. Firtel. 2001. Role of phosphatidylinositol 3′ kinase and a downstream pleckstrin homology domain-containing protein in controlling chemotaxis in *Dictyostelium. J. Cell Biol.* 153:795–809.

Funamoto, S., R. Meili, S. Lee, L. Parry, and R.A. Firtel. 2002. Spatial and temporal regulation of 3-phosphoinositides by PI 3-kinase and PTEN mediates chemotaxis. *Cell.* 109:611–623.

Hirsch, E., V.L. Katanaev, C. Garlanda, O. Azzolino, L. Pirola, L. Silengo, S. Sozzani, A. Mantovani, F. Altruda, and M.P. Wymann. 2000. Central role for G protein-coupled phosphoinositide 3-kinase gamma in inflammation. *Science.* 287:1049–1053.

Hoeller, O., and R.R. Kay. 2007. Chemotaxis in the absence of PIP3 gradients. *Curr. Biol.* 17:813–817.

Iijima, M., and P. Devreotes. 2002. Tumor suppressor PTEN mediates sensing of chemoattractant gradients. *Cell.* 109:599–610.

Janetopoulos, C., T. Jin, and P. Devreotes. 2001. Receptor-mediated activation of heterotrimeric G-proteins in living cells. *Science.* 291:2408–2411.

Janetopoulos, C., L. Ma, P.N. Devreotes, and P.A. Iglesias. 2004. Chemoattractant-induced phosphatidylinositol 3,4,5-trisphosphate accumulation is spatially amplified and adapts, independent of the actin cytoskeleton. *Proc. Natl. Acad. Sci. USA.* 101:8951–8956.

Keizer-Gunnink, I., A. Kortholt, and P.J.M. Van Haastert. 2007. Chemoattractants and chemorepellents act by inducing opposite polarity in phospholipase C and PI3-kinase signaling. *J. Cell Biol.* 177:579–585.

Konijn, T.M. 1970. Microbiological assay for cyclic 3′,5′-AMP. *Experientia.* 26:367–369.

Lee, S., F.I. Comer, A. Sasaki, I.X. McLeod, Y. Duong, K. Okumura, J.R. Yates III, C.A. Parent, and R.A. Firtel. 2005. TOR complex 2 integrates cell movement during chemotaxis and signal relay in *Dictyostelium. Mol. Biol. Cell.* 16:4572–4583.

Loovers, H.M., M. Postma, I. Keizer-Gunnink, Y.E. Huang, P.N. Devreotes, and P.J.M. van Haastert. 2006. Distinct roles of PI(3,4,5)P3 during chemoattractant signaling in *Dictyostelium*: a quantitative in vivo analysis by inhibition of PI3-kinase. *Mol. Biol. Cell.* 17:1503–1513.

Mato, J.M., A. Losada, V. Nanjundiah, and T.M. Konijn. 1975. Signal input for a chemotactic response in the cellular slime mold *Dictyostelium discoideum. Proc. Natl. Acad. Sci. USA.* 72:4991–4993.

Meili, R., C. Ellsworth, and R.A. Firtel. 2000. A novel Akt/PKB-related kinase is essential for morphogenesis in *Dictyostelium. Curr. Biol.* 10:708–717.

Parent, C.A., B.J. Blacklock, W.M. Froehlich, D.B. Murphy, and P.N. Devreotes. 1998. G protein signaling events are activated at the leading edge of chemotactic cells. *Cell.* 95:81–91.

Pitt, G.S., N. Milona, J. Borleis, K.C. Lin, R.R. Reed, and P.N. Devreotes. 1992. Structurally distinct and stage-specific adenylyl cyclase genes play different roles in *Dictyostelium* development. *Cell.* 69:305–315.

Postma, M., L. Bosgraaf, H.M. Loovers, and P.J.M. Van Haastert. 2004. Chemotaxis: signalling modules join hands at front and tail. *EMBO Rep.* 5:35–40.

Roelofs, J., and P.J.M. van Haastert. 2002. Characterization of two unusual guanylyl cyclases from *Dictyostelium. J. Biol. Chem.* 277:9167–9174.

Roelofs, J., M. Meima, P. Schaap, and P.J.M. van Haastert. 2001. The *Dictyostelium* homologue of mammalian soluble adenylyl cyclase encodes a guanylyl cyclase. *EMBO J.* 20:4341–4348.

Sasaki, A.T., C. Janetopoulos, S. Lee, P.G. Charest, K. Takeda, L.W. Sundheimer, R. Meili, P.N. Devreotes, and R.A. Firtel. 2007. G protein–independent Ras/PI3K/F-actin circuit regulates basic cell motility. *J. Cell Biol.* 178:185–191.

Servant, G., O.D. Weiner, P. Herzmark, T. Balla, J.W. Sedat, and H.R. Bourne. 2000. Polarization of chemoattractant receptor signaling during neutrophil chemotaxis. *Science.* 287:1037–1040.

Swanson, J.A., and D.L. Taylor. 1982. Local and spatially coordinated movements in *Dictyostelium discoideum* amoebae during chemotaxis. *Cell.* 28:225–232.

Takeda, K., A.T. Sasaki, H. Ha, H.A. Seung, and R.A. Firtel. 2007. Role of phosphatidylinositol 3-kinases in chemotaxis in *Dictyostelium. J. Biol. Chem.* 282:11874–11884.

Traynor, D., J.L.S. Milne, R.H. Insall, and R.R. Kay. 2000. Ca2+ signalling is not required for chemotaxis in *Dictyostelium. EMBO J.* 19:4846–4854.

Valkema, R., and P.J. Van Haastert. 1992. Inhibition of receptor-stimulated guanylyl cyclase by intracellular calcium ions in *Dictyostelium* cells. *Biochem. Biophys. Res. Commun.* 186:263–268.

Van Haastert, P.J.M., and P.N. Devreotes. 2004. Chemotaxis: signalling the way forward. *Nat. Rev. Mol. Cell Biol.* 5:626–634.

Van Haastert, P.J.M., and M. Postma. 2007. Biased random walk by stochastic fluctuations of chemoattractant-receptor interactions at the lower limit of detection. *Biophys. J.* 93:1787–1796.

Van Haastert, P.J.M., I. Keizer-Gunnink, and A. Kortholt. 2007. Essential role of PI 3-kinase and phospholipase A2 in *Dictyostelium* chemotaxis. *J. Cell Biol.* 177:809–816.

Veltman, D.M., and P.J.M. Van Haastert. 2006. Guanylyl cyclase protein and cGMP product independently control front and back of chemotaxing *Dictyostelium* cells. *Mol. Biol. Cell.* 17:3921–3929.

Wang, F., P. Herzmark, O.D. Weiner, S. Srinivasan, G. Servant, and H.R. Bourne. 2002. Lipid products of PI(3)Ks maintain persistent cell polarity and directed motility in neutrophils. *Nat. Cell Biol.* 4:513–518.

Ward, S.G. 2004. Do phosphoinositide 3-kinases direct lymphocyte navigation? *Trends Immunol.* 25:67–74.

Ward, S.G. 2006. T lymphocytes on the move: chemokines, PI 3-kinase and beyond. *Trends Immunol.* 27:80–87.

Xu, J., F. Wang, A. Van Keymeulen, P. Herzmark, A. Straight, K. Kelly, Y. Takuwa, N. Sugimoto, T. Mitchison, and H.R. Bourne. 2003. Divergent signals and cytoskeletal assemblies regulate self-organizing polarity in neutrophils. *Cell.* 114:201–214.